

Automated evaluation of lung health in covid-19 patients using x-ray scans and enhanced bilateral convolutional neural networks: Potential for lung cancer detection

Tarang Bhatnagar¹, K G Patel², Prashant Rajaram Patil³, Asha K⁴, Sudhanshu Dev⁵, Sumit Tripathi⁶

¹ Centre of Research Impact and Outcome, Chitkara University, Rajpura, Punjab, India

² Department of Biotechnology, Parul University, Vadodara, Gujarat, India

³ Department of Radiology, Krishna Institute of Medical Sciences, Maharashtra, India

⁴ Department of Life Science, School of Sciences, Jain (Deemed to be University), Bangalore

⁵ Chitkara Centre for Research and Development, Chitkara University, Himachal Pradesh, India

⁶ Department of UGDx, ATLAS SkillTech University, Mumbai, Maharashtra, India

ABSTRACT

Background: In December 2019, the rare Coronavirus Disease (COVID-19) pandemic first appeared in Wuhan, China. Life, health and the international economy have all been severely impacted. Timely diagnosis, appropriate staging, and early treatment are the goals for inpatients with COVID attacks. The arrival of the COVID-19 pandemic changed the scenario of screening and diagnosis to stop the outbreak and treat patients rapidly for rapid detection of positive cases, especially those who are suffering from several lung diseases, including lung cancer, which must be detected early.

Objective: Research is to propose Enhanced Bilateral Convolutional Neural Networks (EBCNN) as a means of automating the assessment of the pulmonary health of Covid-19 participants utilizing X-ray images.

Methods: In this study, the CXR image dataset were collected. The acquired X-ray images provide variety and depth to the categorization. The variation in mean values across the groups conducted unpaired, 2-tailed t-tests for statistical analysis. To measure the accuracy of the classifiers, the ROC curve was plotted.

Result: In this investigation, the real-time object identification system's classifier was the EBCNN model. The research shows that EBCNN outperforms standard techniques in terms of F1 score, accuracy and recall.

Conclusion: The approach can be used to help radiologists validate their first patient scanning and can also be used through the cloud to significant health risks right away. The results demonstrate that all classifiers work with the obtaining accuracy score of over 98.5%.

Keywords: COVID-19, lung health, lung cancer, x-ray scans, Enhanced Bilateral Convolutional Neural Networks (EBCNN)

Address for correspondence:

Tarang Bhatnagar

Centre of Research Impact and Outcome, Chitkara University, Rajpura, Punjab, India

E-mail: tarang.bhatnagar.rop@chitkara.edu.in

Word count: 3669 **Tables:** 02 **Figures:** 07 **References:** 17

Received: 14 August, 2024, Manuscript No. OAR-24-147160

Editor assigned: 17 August, 2024, Pre-QC No. OAR-24-147160(PQ)

Reviewed: 01 September, 2024, QC No. OAR-24-147160(Q)

Revised: 08 September, 2024, Manuscript No. OAR-24-147160(R)

Published: 16 September, 2024, Invoice No. J-147160

INTRODUCTION

Severe Acute Respiratory Syndrome Coronavirus 2 (SARS-CoV-2) is the novel coronaviruses causing sickness this year. It has been quickly spreading across China and other nations since December 2019. On June 8th 2020, the global number of confirmed cases was 6931,000, including 400,857 fatalities. T lymphocytes produce antiviral cytokines in reaction to SARS-CoV-2 binding to ACE2 receptors and these cytokines have recently been cleared from the pulmonary septa as well as interstitial regions of the lung. Nevertheless, in sequence on the outcomes of SARS-CoV-2 illness is completely lacking [1]. Neither the prevalence nor the potential impact of COVID-19 pneumonia on pulmonary purpose or HRQoL in survivors has been studied. Despite the absence of data, patients with COVID-19 pneumonia should continue to have their breathing systems closely monitored. According to Chinese research, around partially of all patients with non-hazard COVID-19 pneumonia showed decreased diffusion capacity both on the day they were discharged and again 30 days afterward [2]. Symptoms of this condition include a dry, hacking cough, weakness, difficulty breathing and a loss of taste and smell. On the flip side, problems such as septic shock, ARDS and coagulation malfunction could emerge a week after the initial symptoms manifest. COVID-19 symptoms have been reported across the age spectrum. Those over the age of 30 have the highest incidence of developing the illness, and those who do tend to have more severe symptoms. Early detection of infected individuals is crucial in the struggle beside COVID-19, as are the completion of treatment protocols for severe cases and the implementation of quarantine measures to prevent the spread of infection [3]. Due to the absence of a cure or effective antiviral immunizations, it is crucial to diagnose and monitor patients early to ensure optimal customization of therapy and a reduction in Covid-19-related mortality. Radiologists should go as quickly as feasible through the evaluation and provide trustworthy reports of their findings to determine whether or not the radiological findings are compatible with the illness. Due to the high rate of false-positive results from swab testing, intelligent systems that really can autonomously recognize Covid-19 from CXR images and provide doctors with a diagnostic test would have paramount value [4]. To automatically diagnose sickness from CXR images, a brand-new layered CNN model was created

in the study [5]. During training, the suggested technique generated many sub-models based on the VGG19 and Xception models. To extract image attributes that can be fed into a designated classifier for prediction, the study suggested a deep learning fusion framework built with CNN that employ the domain adaptation principle to unite the parameters (weights) of multiple methods into a solitary system [6]. To distinguish between CXR from well persons and those with pneumonia, a Deep Convolutional Network-based classification system named COVDC-Net was developed in the study [7]. A multi-objective optimization and deep learning-based approach were developed in the study to detect coronavirus infection in X-rays. Several methods of assessing X-ray images for automated COVID-19 analysis are examined and evaluated in [8, 9]. They showed that similar results may be obtained utilizing X-Ray images that exclude mainly lungs. A deep meta-learning-based AI system was presented in research to speed up the processing of CXR images for the automated recognition of COVID-19 patients [10]. They offer supplementary methods for predicting COVID-19 instances by using a Siamese network and contrastive training in tandem to generate unbiased visual characteristics. The research created a robust unsupervised framework for categorizing lung illnesses from CXR and CT images [11]. To produce interpretable representations of images of lung illness, our technique generates multi-layer generative adversarial networks, or Lung-GANs, which can be trained using only unlabeled data.

Research demonstrated a COVIDetectioNet model, an expert-designed system that uses features chosen from a mixture of deep characteristics to diagnose COVID-19 [12]. This research proposes an EBCNN model for automated COVID-19 diagnosis. The suggested method has a continuous structure, provides a diagnosis from unedited chest X-rays, and does not rely on any feature extraction methods. Chest X-ray scans that weren't taken properly and quickly were used to train this model.

The remaining of this paper is planned as follows:

- Section 2 presents the recommended reading list and methodology.
- Section 3 contains the experimental analysis.
- The discussion is in Section 4.
- The conclusion is in Part 5.

METHODS

Circumstances like pneumonia, emphysema and pulmonary disease are diagnosed and treated with the help of chest X-rays by medical professionals. Chest X-rays (CXR) provide a quick, painless diagnosis. After a day or two, you should get the results of your X-ray. A CXR utilizes a narrow ray of emission to examine the organs and bones in the chest. Figure 1 depicts the proposed methodological flow.

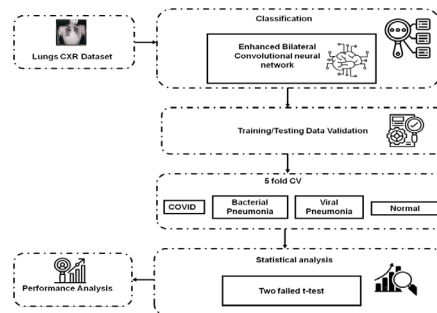


Fig. 1. Protocol for the suggested process

Dataset

CXR imaging files were obtained from Kaggle <https://www.kaggle.com/datasets/prashant268/chest-xray-covid19-pneumonia> [13]. The acquired X-ray images provide variety and depth to the categorization and performance evaluation phase: The dataset comprises 6,432 chest X-ray scans

from an open-source collection of persons with COVID-19, pneumonia and healthy individuals. Table 1 provides information on the CXRimages in the datasets. The CXR images in database are used to generate a train and test set.

Tab. 1. CXR images dataset	COVID-19		Normal		VP		Total
	Training	Testing	Training	Testing	Training	Testing	
	460	116	1266	3418	317	855	6,432

Enhanced Bilateral Convolutional Neural Networks (EBCNN)

EBCNN was one example of the many fine-grained approaches. In EBCNN, an image is represented by a bilinear value that is the outer product of values from 2 CNNs. Just the racially biased value is used, and the approach's tight granularity allows the

bilinear feature to be used to find and identify the localized initial feature relationships. If the bilinear operation is seen as a parameter less identity process, training might be much simplified. To diagnose NF1-S, to created original AI methods like EBCNN. As NF1-S diagnosis is so challenging and important, the strategy is geared at spotting subtle characteristics.

It was inspired by the current attention that bilinear operation has received. The findings of the diagnostic are produced by EBCNN using the chest x-ray images as inputs. As previously

indicated, to produce EBCNN to extract the bilinear-like structures from chest x-ray images. The technique is modeled after EBCNN in figure 2.

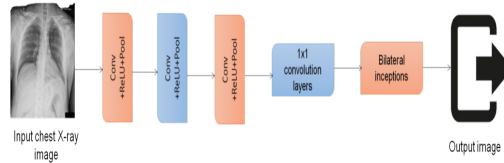


Fig. 2. Structure of EBCNN

EBCNN

It effectively generated a bilinear feature using the j^{th} patient's chest x-ray image. In particular, to created

$$e_B(v_j) \in \mathbb{R}^{C \times K} \text{ and } e_A(v_j) \in \mathbb{R}^{C \times K}$$

using the outputs of 2 CNNs. where A stood for the outputs' width, K for the locations as well as $e(*)$ for the VGG-16 convolutional layers. The bilinear component at point k might then be generated in the manner shown below:

$$bilinear(k, v_j, e_B, e_A) = e_B(k, v_j) e_A(k, v_j)^T \quad (1)$$

By combining the bilinear mixture of the properties overall placed in the image and then the desired direction as follows, it is possible to create the worldwide bilinear

$$\text{form } a_j^{EBCNN} \in \mathbb{R}^{C \times C} \\ a_j^{EBCNN} = \sum_{k=1}^K bilinear(k, v_j, e_B, e_A) \quad (2)$$

To combined the values of $e_B(.)$ and $e_A(.)$, which further increased efficiency while maintaining performance parity with the cases when an $a_j^{ADMM} \in \mathbb{R}^{C \times C}$. Now, the following is the bilinear expression $e_B \neq e_A$:

$$a_j^{single} = \sum_{k=1}^K bilinear(k, v_j, e_B, e_A) \quad (3)$$

In contrast to that surgeons normally utilize chest x-ray images for accurate diagnosis; In a CXR image, EBCNN succeeds in locating the perfectly alright effective increase for a diagnosis.

To adopted the EBCNN for use with CXR images and projected 2-path EBCNN so that the full potential of the images' rich information could be realized. Double-path EBCNN As previously noted, to merge the data from 2 distinct x-ray images of patient j collected from different angles, the 2-path bilinear factor an $a_j^{two} \in \mathbb{R}^{C \times C}$ was obtained by computing the bilinear features of each image and then combining them individually.

$$a_j^{two} = \sum_{k=1}^K bilinear(k, v_j^d, e_B, e_B) + \sum_{k=1}^K bilinear(k, v_j^l, e_B, e_B) \quad (4)$$

By doing this, were able to maintain and align the location data of each image, as well as EBCNN then took into account their correlations worldwide. Moreover, induced the 2 streams to collect

comparable characteristics for the diagnosis by conducting element-wise addition on them.

In actuality, the features might be extracted from several viewpoints using 2-path EBCNN. Nevertheless, it did not take into account how the features interacted with one another; it just added the features. To solve this issue introduced EBCNN, which, as shown below, used bilinear operations to identify comparable characteristics in two x-ray images.

This technique generated bilateral characteristics that matched the shared areas of interest in 2 CXR images from the j^{th} patient's CXR images, v_j^d , and v_j^l . In particular, the following can be done to get the bilateral bilinear representation $a_j^{bilateral} \in \mathbb{R}^{C \times C}$:

$$a_j^{bilateral} = \sum_{k=1}^K bilinear(k, v_j^d, e_B, e_B) = \sum_{k=1}^K e_B(k, v_j^d) e_A(k, v_j^l)^T \quad (5)$$

Large values inside the outer combination of the parameters derived from the chest x-ray images showed similar regions of interest, highlighting the images' racially biased components needed to diagnose NF1-S. That is to say, by emphasizing the same factors, EBCNN was able to capture the correlations between the chest x-ray images.

Training and testing data formulation

The training and testing of sample construction and modeling were done using the Jack-knife fivefold Cross-Validation (CV) approach. It is one of the most well-known, often used, and productive techniques for employing a fivefold CV to validate the accuracy of a classifier. The samples for the remaining folds are categorized into classes according to the instruction conducted on the fourfold, and the data are separated into five folds for training. The samples collected in the testing fold are completely invisible to the trained models. Five times during the whole procedure, each class sample is categorized by the results. Last but not least, the classified labels for the unseen samples will be used to assess classification performance.

Statistical analysis

Statistical tests for detecting differences across groups were unpaired, 2-tailed, and of unequal variance. Pneumonia due to

COVID-19 served regular Receiver-Operating Characteristic (ROC) curve investigation, whereas pneumonia due to bacteria and viruses apart from COVID-19 served as the diagnostic test. Using the usual ROC analysis, the performance was assessed for sensitivity, specificity, and accuracy, as well as significance with the p value. AUC was tabulated with lower and upper limits and accuracy. The statistical analysis was done using MATLAB.

Experimental analysis

The suggested model is worked in MATLAB and its efficiency is contrasted with that of other methods, including Deep Convolutional Neural Networks (DCNN), CNN and Logistic Regression with Convolution Neural Networks (LR-CNN) [14-16]. Performance indicators including accuracy, F1-score, and recall were examined using the suggested and existing approaches. As for the X-ray abnormalities, educated a DL methods, EBCNN, to distinguish between Pneumonia, COVID-19 and

Normal. It has also been shown that the EBCNN model can tell the difference between COVID-19 and Normal. For both, bi and tri classification issues, the suggested method efficiency are examined by 5-fold cross-validation. Around 80% of all X-rays are put to educational use, whereas 20% are for validation. All of the folded k pieces have been arranged and are waiting to be used in the verification process. To train the EBCNN, 100 epochs were employed.

Figure 3 depicts the EBCNN model in fold-1. Loss values increase early on in training but drop down precipitously later on. This unexpected increase and decrease may be attributed, in large part, to the fact that the COVID-19 class has fewer data to work with than the other 2 (Pneumonia and No-Findings). But, when training progresses and all epoch's X-ray images are re-analyzed by the deep model, the rapid oscillations weaken.

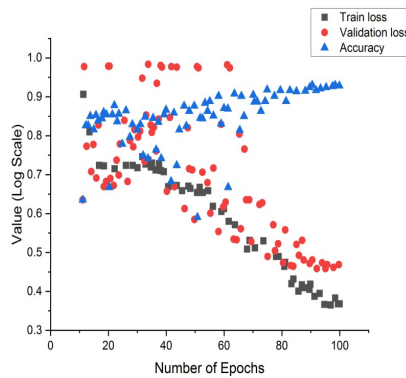


Fig. 3. EBCNN model in fold-1

$$Accuracy = \frac{TP+TN}{TP+FP+FN+TN} \tag{6}$$

$$Recall = \frac{True\ positive}{total\ number\ of\ actual\ positives} \tag{7}$$

$$F1\ SCORE = 2 \times \frac{Precision*recall}{Precision+recall} \tag{8}$$

Figure 4 displays the accuracy of the recommended and existing methods. It is the percentage of all model predictions that were accurate across all test samples. To divide the sum of responses by the total number of correctly recognized ones to evaluate if a statement is true. It was shown that the suggested EBCNN methodology outperformed the existing techniques, such as DCNN, CNN, and LR-CNN.

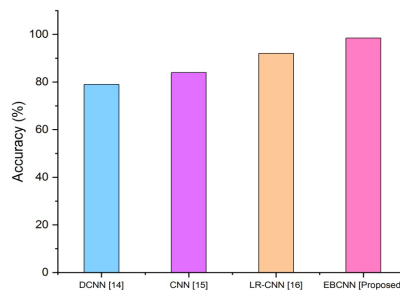


Fig. 4. Comparison of the accuracy

Figure 5 displays the recall of the recommended and present methods. The recall is a metric utilized to evaluate how successfully medical device data systems can track down the additional information needed for an individual. It has been found that the following actions are crucial. It has been shown

that in terms of memory, capacity to identify, and land cover supporting images, the proposed approach, EBCNN, surpasses modern methods like DCNN, CNN, and LR-CNN.

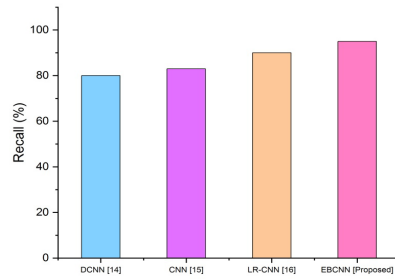


Fig. 5. Recall of proposed and existing methods

The comparison of the F1-score is shown in figure 6. The F1 score also considers accuracy and memory. The incidence signifies is the center or average of expected values. It has been argued that the waveform resources, a distinct model of manipulative a

standard of numbers, are better suitable for ratios than the conventional arithmetical distributions. The proposed EBCNN approach outperforms the presently used DCNN, CNN, and LR-CNN methods in terms of the F1 score.

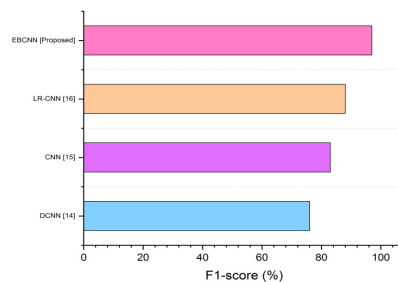


Fig. 6. F1-score of proposed and existing methods

Figure 7 depicts the ROC curve. A ROC curve shows the genuine Sensitivity *vs.* the the100-Specificity. Every spot on the ROC plot represents a specificity and sensitivity pair connected with a different decision level. When there is no concordance between

the 2 distributions, a perfect ROC map indicates that the test can discriminate between them. The proposed EBCNN approach outperformed the presently used DCNN, CNN, and LR-CNN methods in terms of the ROC curve.

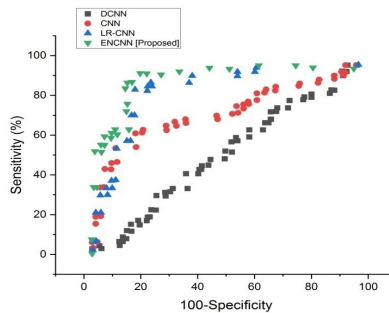


Fig. 7. ROC curve

In table 2, the proposed method performance analysis is condensed. A randomly selected associate of the optimistic set will, 87% of the time, have a superior test result than a randomly selected member of the negative group, according to an AUC of 0.87. An AUC of 0.5 indicates that because the distributions of the 2 groups are the same, the variable is unable to distinguish

between them. An AUC of 1, on the other hand, indicates total group separation with no distribution overlap. The test can successfully discriminate between the groups if the 95% confidence interval does not include 0.5, which is the hypothesis for an AUC of 0.5.

Tab. 2. Performance analysis of the EBCN	CXR data	AUC (95% CI)	t-value	p-Value
	COVID-19	0.88 (0.85-0.91)	3.5	<0.001
	Normal	0.72 (0.68-0.76)	2.8	<0.002
	Pneumonia	0.81 (0.78-0.84)	3.2	<0.001

DISCUSSION

The measures illustrate that the suggested model outperforms the existing models, which has a lot of deep issues. Listed below are some of the issues with the current approach. In hopes of creating a precise model for the diagnosis of the disease, Dr. Cohen collected radiological images from COVID-19 patients. This source provided COVID-19 image data for much of this study [14]. For other studies, such as those that employed non-COVID-19, images were sourced from a variety of publically accessible sources. Nevertheless, non-COVID photos in this research are those of kids among the ages of 1 year and 5 years old. Additionally, the researchers experimented with various models and methodologies in combination. ResNet50 were images to reach an accuracy of 95.38 percent. It used CT scans and deep methods called DRE-Net that was based on the pre-trained ResNet50 to obtain an 86% success rate [15]. The classification accuracy was 82.9% using CT scans and a deep network based on a modified version of the Inception architecture (M-Inception). Using the described 3D deep CNN model, they were able to successfully identify COVID-19 from CT images 90.8% of the time. ResNet, when used in combination with CT scans, had an 86.7% success rate in identifying COVID-19. Most of these studies don't have enough information to construct a reliable model [16]. Moreover, a rigorous screening procedure is necessary to exclude irrelevant photographs from the archive. As the COVID-19 pandemic is still quite recent, there aren't as many X-rays accessible for AI to analyze [17].

X-ray radiographs can now be used in the diagnosis of COVID-19 due to the suggested paradigm shift. Because of their widespread availability, X-ray radiographs are often used in the diagnostic process. They are in high demand in hospitals all across the world because of the current pandemic. In a couple of seconds, the model can detect COVID-19. CT is a costly and inconvenient technique since it is often only available at larger hospitals. However, a CT scan exposes the patient to more radiation than an X-ray does. Hence, X-ray images should be utilized with a DL model since they are easier to get and expose patients to less radiation than CT scans. Individuals who are recognized by the methods as having COVID positivity may be

sent to specialized facilities for confirmation and immediate treatment.

CONCLUSION

It was suggested in this research to use the EBCNN to identify and categorize cases of COVID-19 in CXR images. Because of its comprehensive design and level of automation, this model does leave with the requirement for human intervention in the characteristic mining process. This experiment looked at a wide range of metrics, including recall, F1-score, accuracy, and ROC curve. The results of the suggested EBCNN were 98.5% accuracy, 95% recall, and 97% F1 score. The suggested approach outperforms the current approaches. Expert radiologists evaluate the built model's performance, and it is now prepared for testing with a bigger database. To get around a lack of radiologists in rural areas of COVID-19-affected nations, employ this technique. Additionally, these models can be used to identify other conditions affecting the chest, such as pneumonia and tuberculosis. One disadvantage of the research is that only an incomplete integer of X-ray images from COVID-19 were used.

The goal is to fortify and refine our model's accuracy by including more, analogous images from local hospitals. To Plan on expanding the model with more supporting visuals shortly. This produced model can be stored in the cloud and utilized for timely patient diagnosis and to facilitate a speedy recovery. This should make the doctors' jobs much easier. This model would like to be implemented in the scenario of oncology and might be useful to oncologists for understanding the stage or degree of progression of the metastasis of lung cancer patients. To compare the results achieved using a model created and trained on X-ray images to those acquired using CT scans for COVID-19 detection. Also gather regional radiology images of patients with COVID-19 from hospitals throughout Turkey to analyze using the model. When the required testing is completed, want to introduce the created model for screening in nearby general and lung cancer hospitals.

REFERENCES

1. Zhao YM, Shang YM, Song WB, Li QQ, Xie H, et al. Follow-up study of the pulmonary function and related physiological characteristics of COVID-19 survivors three months after recovery. *EClinicalMedicine*. 2020;25:100463.
2. Talman S, Boonman-de Winter LJ, De Mol M, Hoefman E, Van Etten RW, et al. Pulmonary function and health-related quality of life after COVID-19 pneumonia. *Respir Med*. 2021;176:106272.
3. Alhudhaif A, Polat K, Karaman O. Determination of COVID-19 pneumonia based on generalized convolutional neural network model from chest X-ray images. *Expert Syst Appl*. 2021;180:115141.
4. Duong LT, Nguyen PT, Iovino L, Flammini M. Automatic detection of Covid-19 from chest X-ray and lung computed tomography images using deep neural networks and transfer learning. *Appl Soft Comput*. 2023;132:109851.
5. Gour M, Jain S. Automated COVID-19 detection from X-ray and CT images with stacked ensemble convolutional neural network. *Biocybern Biomed Eng*. 2022;42:27-41.
6. Shorfuzzaman M, Masud M, Alhumyani H, Anand D, Singh A. Artificial neural network-based deep learning model for COVID-19 patient detection using X-ray chest images. *J Healthc Eng*. 2021;2021:1-6.
7. Sharma A, Singh K, Koundal D. A novel fusion-based convolutional neural network approach for classification of COVID-19 from chest X-ray images. *Biomed Signal Process Control*. 2022;77:103778.
8. Dhiman G, Chang V, Kant Singh K, Shankar A. Adopt: automatic deep learning and optimization-based approach for detection of novel coronavirus COVID-19 disease using X-ray images. *J Biomol Struct Dyn*. 2022;40:5836-5847.
9. Maguolo G, Nanni L. A critic evaluation of methods for COVID-19 automatic detection from X-ray images. *Inf Fusion*. 2021;76:1-7.
10. Shorfuzzaman M, Hossain MS. MetaCOVID: A Siamese neural network framework with the contrastive loss for n-shot diagnosis of COVID-19 patients. *Pattern Recognit*. 2021;113:107700.
11. Yadav P, Menon N, Ravi V, Viswanathan S. Lung-GANs: unsupervised representation learning for lung disease classification using chest CT and X-ray images. *IEEE Trans Eng Manag*. 2021.
12. Turkoglu M. COVIDetectioNet: COVID-19 diagnosis system based on X-ray images using features selected from pre-learned deep features ensemble. *Appl Intell*. 2021;51:1213-1226.
13. Kaggle. Chest X-ray images.
14. Wang L, Lin ZQ, Wong A. Covid-net: A tailored deep convolutional neural network design for detection of covid-19 cases from chest x-ray images. *Sci Rep*. 2020;10:1-2.
15. Hassantabar S, Ahmadi M, Sharifi A. Diagnosis and detection of infected tissue of COVID-19 patients based on lung X-ray image using convolutional neural network approaches. *Chaos Solitons Fractals*. 2020;140:110170.
16. Rasheed J, Hameed AA, Djeddi C, Jamil A, Al-Turjman F. A machine learning-based framework for the diagnosis of COVID-19 from chest X-ray images. *Interdiscip Sci Comput Life Sci*. 2021;13:103-117.
17. Gupta S, Shabaz M, Vyas S. Artificial intelligence and IoT-based prediction of Covid-19 using chest X-ray images. *Smart Health*. 2022:100299.